Available online at www.sciencedirect.com
SCIENCE DIRECT®
Carbohydrate Research 339 (2004) 301–312
Carbohydrate RESEARCH

NMR structural determination of dissolved O-acetylated galactoglucomannan isolated from spruce thermomechanical pulp

Tea Hannuksela[a,*] and Catherine Hervé du Penhoat[b,†]

[a]*Process Chemistry Group, Åbo Akademi University, Porthaninkatu 3, FIN-20500 Turku/Åbo, Finland*
[b]*Centre de Recherches sur les Macromolécules Végétales, CNRS (affiliated with University Joseph Fourier), BP 53, 38041 Grenoble Cedex 9, France*

Received 6 May 2003; received in revised form 13 August 2003; accepted 9 November 2003

Abstract—Water-soluble O-acetylated galactoglucomannan (GGM) isolated from spruce thermomechanical pulp (TMP) by hot-water extraction was characterized by 1D and 2D (homo- and heteronuclear) NMR analysis. The backbone was found to consist of (1→4)-linked mannopyranosyl and glucopyranosyl units in a ratio of 10:1.9–2.6. The mannopyranosyl units were acetylated at C-2 and C-3 with a degree of acetylation around 0.28–0.37 as determined by NMR. A slightly larger amount of 2-O-acetylated mannopyranosyl was detected when compared to the 3-O-acetylated component. Approximately every 10th mannopyranosyl unit was substituted at C-6 by a single α-galactopyranosyl unit. Fine structure determination based on sequence-specific chemical shift variations showed that the distribution of glycosyl residues is random. Small amounts of other minor polysaccharide species including xylans and galactans could also be identified by NMR.

Keywords: Galactans; Galactoglucomannans; *O*-acetyl groups; Spruce; TMP; Xylans

1. Introduction

Galactoglucomannans (GGMs) have been extensively studied throughout the years, initially because of their abundance and importance in the pulp and paper industry.[1] More recently, fundamental knowledge of the composition and role of mannans in plant cell walls, as well as new interesting application of mannans for industrial use have been explored. GGM is the dominating hemicellulose group in spruce wood.[2,3] It has been proposed to consist of a main chain of (1→4)-linked β-D-mannopyranosyl units interspersed with a lower number of (1→4)-linked β-D-glucopyranosyl units. Single (1→6)-linked α-galactopyranosyl units are found as side groups branched to the mannopyranosyl units. In softwood, the GGMs are believed to be O-acetylated at C-2 and C-3 of the mannosyl units. GGMs are also found in other wood species as well as in the primary cell walls of other plants, fruits, and seeds, such as flax,[4] tobacco plants,[5] or kiwifruit.[6]

Spruce wood is widely used in mechanical pulping, that is, high yield pulping, where none of the wood constituents are intentionally removed from the pulp. Studies in our laboratory have shown that dissolved GGMs play an important role in mechanical pulping and papermaking.[7–9] During refining of wood, several wood constituents are released into the process water. Most of the dissolved GGMs are, however, removed from solution through sorption onto fiber surfaces, either due to deacetylation (decreased solubility) of the mannan during alkaline peroxide bleaching,[7] or due to introduction of chemical pulps as reinforcement fibers, which, because of their high cellulose content, preferentially sorb mannans.[10] GGM sorption ameliorates the paper strength properties in addition to increasing the yield.[9] Dissolved GGMs are, furthermore, interacting

* Corresponding author. Tel.: +358-2-215-4233; fax: +358-2-215-4868; e-mail: tea.hannuksela@abo.fi
† Present address: Department of Chemistry, State University of New York at Buffalo, 807 Natural Sciences Complex, Buffalo, NY 14260, USA.

0008-6215/$ - see front matter © 2003 Elsevier Ltd. All rights reserved.
doi:10.1016/j.carres.2003.10.025

with wood resin droplets, giving them steric stability and lowering their deposition tendency.[11,12] Due to the higher degree of white-water system closure, that is, recycling of the process water inside the mill, the concentration of wood resin in the process waters can become high and deposition more likely.

In order to understand these fundamental and beneficial interactions of GGMs in papermaking, first the fine structure and ultimately the conformational preferences of GGM need to be determined.

Fine structure: NMR analysis is the method of choice for the structural analysis of polysaccharides. It is a fast, reliable, and nondestructive technique. Most wood hemicelluloses including GGMs are rather large polymers and their molar masses are normally reduced before NMR analysis to reduce line broadening (longer T_2 values) and improve detection (shorter T_1 values). Three publications on the NMR structural characterization of acetylated GGMs from spruce in combination with linkage analysis techniques have appeared recently.[13–15] The approach used to isolate the GGMs in the first two papers yielded samples of relatively low molar mass and, in all cases, only partial assignment of the chemical shifts of acetylated spruce GGMs was reported. However, ^{13}C chemical shift variations as a function of triad structure have been demonstrated for the related acetylated glucomannan from *Linum usitatissimum* L.[4] and such data should be very useful for establishing the fine structure of acetylated spruce GGM. In this approach, it is assumed that the chemical shifts of the middle residue of a trisaccharide fragment within a polysaccharide depend only on the nature of the preceding and following sugar units.

The present work focuses on the NMR structural determination of dissolved spruce GGM in its native acetylated form. Our goals were as follows: (1) to complete the ^1H and ^{13}C chemical shift assignments of GGM, (2) to compare the sugar composition of the soluble fraction with that of the total isolated GGM sample, (3) to determine whether the fine structure is best described in terms of a statistical random repeating unit or as an assembly of block-like fragments, (4) to identify the minor polysaccharides that are isolated with GGM, (5) to obtain conformationally dependent NMR parameters, and finally, (6) to conduct a preliminary experimental investigation of GGM/hydrophobic molecule interactions.

2. Results and discussion

2.1. Chemical composition and molar mass

2.1.1. Molar mass. According to the molar mass determinations, the average M_w of the GGM was around 20 kg/mol (kDa), giving a DP of approximately 120, which is in agreement with the literature. The GGM sample used to determine the average M_w was the low molar-mass fraction of the total sample that had passed a 50 μm filter, leaving around 2/3 of the initial GGM on the filter (molar mass of 78 kg/mol). Sjöström[2] proposed for spruce GGM a molar mass of 56–60 kDa, Willför et al.[15] 41–45 kDa, and Capek et al.[13] found it to be 11 kDa (isolated from holocellulose).

2.1.2. Glycosyl composition. The molar ratio of Gal:Glc:Man:Ac determined by GC after acid methanolysis is shown in Table 1. The actual amount of galactose in the GGM polymer is slightly lower due to the presence of other minor wood hemicelluloses as will be discussed below. Moreover, the trace amounts of various sugars (Ara, Rha, Xyl, GalA, and GlcA) are also due to hemicellulose contaminants. The sugar ratios determined from integration of the peaks in the ^1H NMR and ^{13}C NMR spectra of the low molar-mass fraction are furthermore shown in Table 1.

From integration of the individual Man*p* peaks in the 1D NMR spectra, it could be seen that the 2-*O*-AcMan*p* and 3-*O*-AcMan*p* species represented approximately 19–21% and 17–19%, respectively, leaving 60% of the total mannose units nonacetylated. Based on the amount α-galactose, at most 18–22% of the nonacetylated Man*p* residues were 6-substituted leaving half of all Man*p* units nonacetylated and unsubstituted. Capek et al.[13] have reported that the occurrence of $(1\rightarrow6)$-substitution of mannose by α-Gal*p* is four times greater than for glucose.

The degree of acetylation of the Man*p* units (28–37%) determined by NMR for the low molar-mass sample was lower than the one (53%) established by GC analysis. Many of the peaks in the NMR spectrum are overlapping, which makes quantitative determination more difficult. However, it was also conceivable that the higher molar-mass component of the NMR sample was not detected by NMR due to reduced molecular mobility. In fact, comparison of GGM signal intensity

Table 1. The carbohydrate composition (molar ratio) of the isolated spruce GGM sample determined by GC analysis after acid methanolysis and by NMR

	Gal	Glc	Man	Ara	Rha	Xyl	GalA	GlcA	Ac
GC analysis	2.11	2.66	10	0.32	0.06	0.24	0.49	0.11	5.35
^1H NMR	1.3 + 0.6[a]	1.9	10	0.2				0.2	2.8–3
^{13}C NMR	1.1 + 0.5[a]	2.6	10						3.7

[a]This contribution is from the hemicellulose β-galactan contaminents.

with that of an internal standard (DMSO) revealed that only approximately 75% of the total low molar-mass NMR sample could be detected. Capek et al.[13] found that 50% of the mannose units were acetylated while Willför et al.[15] found it to be 65%. The ratio between 2- and 3-*O*-AcMan*p* is, however, not equal. Willför et al.[15] and Capek et al.[13] found that the 2-*O*-AcMan*p* residue was in majority (2.2:1 and 1.7:1, respectively, compared to 1.1–1.2:1 found in the present study). Lundqvist et al.[14] reported equal amounts of 2- and 3-*O*-AcMan*p*, but the total degree of acetylation was, nevertheless, low (DS = 0.33). Willför et al.[15] showed, however, that the molar mass and ratio of the sugar units of isolated GGM depends on isolation time and temperature as well as on the form of wood raw material (pulp or wood).

When comparing the integrals from the carbon spectrum, the Glc*p*/Man*p* ratio was found to be in agreement with the results from GC analysis and it was only the amount of Gal that was considerably lower. The acid methanolysis technique gives, nonetheless, the total galactose content and cannot separate Gal units originating from different hemicelluloses. The 'missing' Gal has been identified in the NMR spectra as separate minor wood polymers (namely β-galactans, vide infra).

2.2. NMR assignments

Nearly 20 different crosspeaks were detected in the anomeric region of the HSQC spectrum (Fig. 1a). ^{1}H and ^{13}C chemical shift data for the corresponding residues were extracted from 2D spectra (HSQC, HMBC, DQCOSY, TOCSY, and ROESY). The sugar units were then identified as specific trisaccharide fragments or triads by comparison of their chemical shifts with those of the literature and these data are collected in Table 2. Sequential information based on ROESY interresidue crosspeaks, and heteronuclear interglycosidic coupling has been given in Table 3. It was also analyzed in terms of triad structure to give a tentative proposal for the fine structure of acetylated GGM.

2.2.1. Mannose. The signals of reducing α- and β-mannnopyranosyl units were easily detected in the anomeric region of the HSQC spectrum through their characteristic crosspeaks at 5.19/94.86 and 4.93/94.72 ppm, respectively. Partial chemical shift correlation data for the α-residue was extracted from the DQCOSY (H-1/H-2 crosspeaks with small $J_{1,2}$) (Fig. 2) and the HMBC (H-1/C-3 and H-1/C-5 at 5.19/69.9 and 5.19/71.85 ppm, respectively) (Fig. 3) spectra. However,

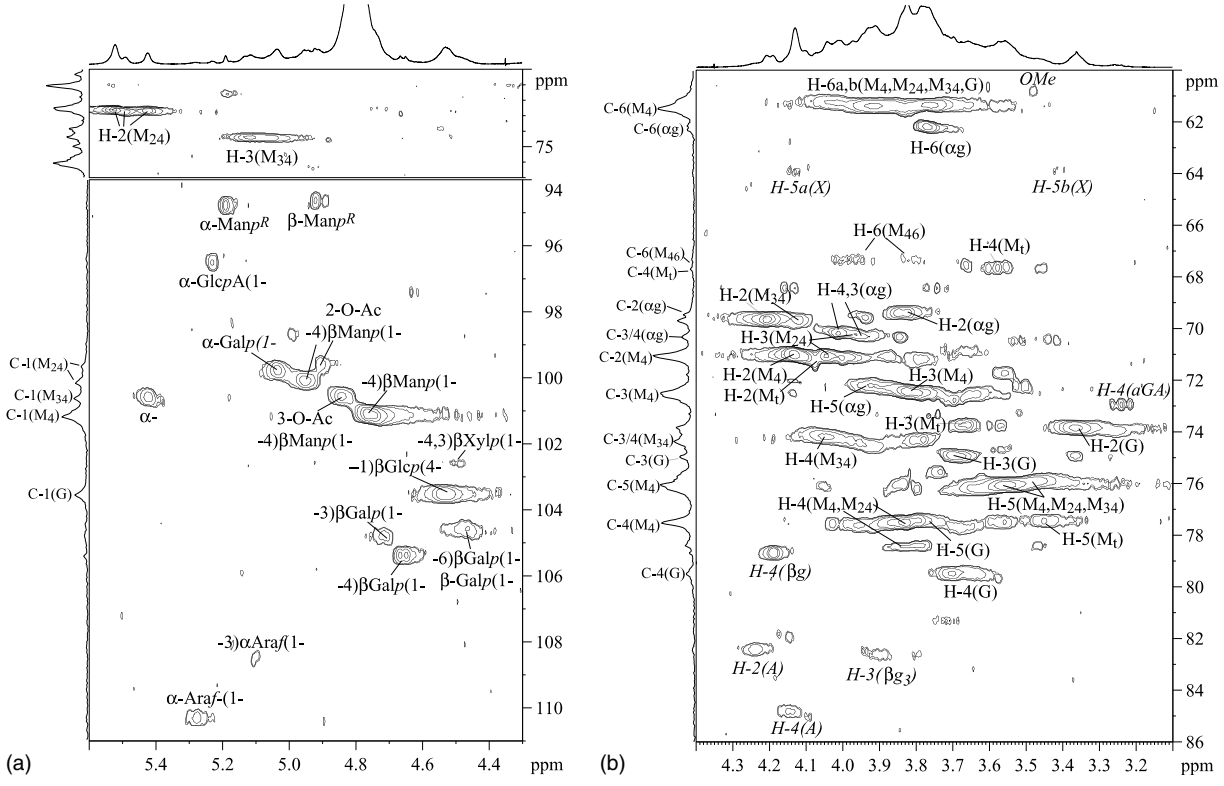

Figure. 1. a and b: HSQC spectrum of the anomeric region (a) and the rest of the spectrum (b) for acetylated GGM. Key: M_{24}, 2-O-acetylated 4-linked Man; M_{34}, 3-O-acetylated 4-linked Man; M_4, nonacetylated 4-linked Man; M_{46}, nonacetylated 4,6-linked Man; M_t, terminal Man; M_R, reducing Man; G, 4-linked Glc; αg, α-Gal*p*-(1→6; βg, 4-linked β-galactan; $βg_3$, 3-linked β-Gal*p*; $βg_6$, 6-linked β-Gal*p*; X, 4-linked Xyl; X_2, 4-linked Xyl substituted at position 2; X_3, 4-linked Xyl substituted at position 3; A, α-Ara*f*-(1→3; αGA, αGlcA (1→2; α, unidentified α-sugar; OMe, 4-*O*-methyl. *Italics* designate sugars not belonging to the GGM polysaccharide.

Table 2. ^{1}H and ^{13}C NMR data for the water-soluble spruce galactoglucomannan

Sugar	H-1 C-1	H-2 C-2	H-3 C-3	H-4 C-4	H-5 C-5	H-6a,b C-6	Triad	Ref.
Mannose								
α-Man*p*^{R} maj	5.19	4.01	3.92 (3.94)					14
	94.86	71.2	69.9[a] (69.6)		71.85[a]			
α-Man*p*^{R} min	5.177	3.97						
	94.86							
→4)-β-Man*p*-(1→, 2-*O*-Ac maj	4.96	5.52	4.03	3.875	3.64[e]	3.94, 3.78[e]	S$\underline{M}_{24}M_x$ or S$\underline{M}_{24}$G	4,14
	100.13	72.63	71.12	77.45	76.2			
→4)-β-Man*p*-(1→, 2-*O*-Ac w	4.94	5.49	3.98	3.85	3.54		$M_{24}\underline{M}_{24}$ M_x or $M_{24}\underline{M}_{24}$G	4,14
	100.13	72.72		78.3	76.1			
β-Man*p*^{R} maj	4.93	4.02	3.82					
	94.72	71.8[a]						
→4)-β-Man*p*-(1→, 2-*O*-Ac min	4.92	5.42	3.99	3.84	3.56		S$\underline{M}_{24}M_{34}$	4,14
	99.78	72.68	71.22	77.6	76.1			
β-Man*p*^{R} min	4.89	3.98						
	94.74							
→4)-β-Man*p*-(1→, 3-*O*-Ac maj	4.84	4.21	5.13	4.05	3.65		S$\underline{M}_{34}M_x$ or S$\underline{M}_{34}$G	4,14
	100.63	69.72	74.39	74.2	76.3			
→4)-β-Man*p*-(1→, 3-*O*-Ac min	4.83	4.19	5.06	4.06	3.57		$M_{24}\underline{M}_{34}M_x$ or $M_{24}\underline{M}_{34}$G	4,14
	100.64	69.72	74.43	74.2	76.12			
→4)-β-Man*p*-(1→, 3-*O*-Ac w	4.82	4.12	5.11	4.03 (3.98)	3.59			
			74.39		76.12			
→4,6)-β-Man*p*-(1→	4.79[b]				3.70[b]	3.94–4.03, 3.79–3.84[f]	X$\underline{M}_{46}$G	16,17
					76.2	67.3		
→4)-β-Man*p*-(1→ maj	4.785	4.13	3.82	3.85	3.56	3.91, 3.76[g]	S$\underline{M}_4M_x$ S$\underline{M}_4$G	4,14
	101.16	71.12	72.50	77.63	76.1	61.50		
β-Man*p*-(1→	4.75	4.076	3.66	3.575	3.45[e]	3.95, 3.735[e]		17
	101.17	71.47	73.76	67.78	77.5	61.9		
→4)-β-Man*p*-(1→min1	4.74	4.102	3.77	3.81	3.46[b]		$M_{24}\underline{M}_4M_x$ or $M_{24}\underline{M}_4$G	4
	101.161	71.15	72.55	78.45	76			
→4)-β-Man*p*-(1→min2	4.726	4.05[b,c]	~3.82[b]	3.79	3.49[b]		S$\underline{M}_4M_{34}$	4
				78.45				
Glucose								
→4)βGlc*p*-(1→maj	4.53	3.364	3.702	3.63	3.78[b]		$M_{46}\underline{G}M_4$[d]	16
	103.57	73.87	74.98	79.519	77.5			18
→4)βGlc*p*-(1→min	4.53	3.35	3.66	3.68				

Galactose							
αGal*p*-(1→	5.038	3.83	3.958	4.01	3.92	3.77	17
	99.84	69.46	70.31	70.26	72.3	62.29	
α-Glycosyl unit							
	5.418	3.645	3.975				16
	100.65	72.61	74.3				

Conditions: 25 °C in D_2O; DMSO internal standard with δ_H and δ_C at 2.74 and 39.74 ppm, respectively. All the proton coupling constant patterns ($^3J_{H\text{-}1,H\text{-}2}$, $^3J_{H\text{-}2,H\text{-}3}$, $^3J_{H\text{-}3,H\text{-}4}$) for the nonreducing residues in the DQCOSY spectrum were as follows: galactose (m,l,m), glucose (m,l,l), mannose (s,m,l), and xylose (m,l,l), where—l, large (8–10 Hz); m, medium (3–5 Hz); s, small (<2 Hz). Key: triad definitions derived from van Hazendonk et al.[4]—G, 4-linked Glc; M_{24}, 2-O-acetylated 4-linked Man; M_{34}, 3-O-acetylated 4-linked Man; M_{46}, nonacetylated 4,6-linked Man; M_x, M_4 or M_{24}; S, any 4-linked monosaccharide except M_{24}; X, unassigned; the values correspond to the underlined residue in the triad; maj, major; min, minor; w, weak.

[a] HMBC.

[b] ROESY (τ_m 100 ms).

[c] TOCSY (τ_m 70 ms).

[d] ROESY (τ_m 200 ms).

[e] TQCOSY.

[f] Only signals in the HSQC spectrum compatible with 6-substitution.

[g] Most intense H-6a,b/C-6 crosspeaks in the HSQC spectrum.

only the H-1/H-2 (TOCSY, 70-ms mixing time) connectivity could be established for β-Man*p*^{R} whose population represents only about 25% of the reducing sugars.[16]

The resonances of the anomeric protons of the (1→4)-linked nonacetylated β-Man*p* residues overlapped with the right shoulder of the residual water peak but the carbon signals of the major component (C-1 101.16 ppm; H-1/H-2 4.785/4.13 ppm) were the strongest ones in the 1D ^{13}C spectrum. A complete set of crosspeaks was observed in the HSQC spectrum and assignments were confirmed by correlations in the DQCOSY (H-1/H-2, H-2/H-3, and H-4/H-5 crosspeaks), TOCSY (mixing time 40 ms—H-1/H-2, H-2/H-3–H-5), ROESY (100-ms mixing time—H-1/H-2, H-1/H-3, H-1/H-5), and HMBC (*J*-filter, 65 ms—H-1/C-2, H-2/C-3, H-2/C-4, H-3/C-1, H-3/C-4, H-4/C-3, H-4/C-5, H-5/C-4) spectra. Other crosspeaks involving the H-1 protons resonating in the 4.72-4.80 ppm region were detected in the homonuclear 2D spectra (H-1/H-2—4.80/4.07, 4.79/?, 4.75/4.076, 4.74/4.102, 4.726/4.05). Partial data were obtained for four (three sets have been collected in Table 2) minor nonacetylated (1→4)-linked β-Man*p* species and a complete set of carbon and protons chemical shifts were detected for the sugar with the sharpest signals. The latter sugar was demonstrated to be the terminal β-Man*p* (1→ residue by comparison of its chemical shift data with those reported for digalactosylmannopentaose.[17] Two groups of nonacetylated β-Man*p* species could be further distinguished based on the H-5 chemical shifts: two 4-linked units with $\delta_{H\text{-}5}$ lower than 3.60 ppm (H-1 resonating at 4.74 and 4.726 ppm) and a likely candidate for 4,6-linked β-Man*p* ($\delta_{H\text{-}1}$ at 4.79 ppm) with a ROESY crosspeak at 4.79/3.70, identical to the H-1/H-5 chemical shifts of 4,6-linked β-Man*p* in GGM from suspension-cultured cells[16] and analogous to those of 4,6-linked β-Man*p* (4.766/3.767 and 4.772/3.755 ppm) in the aforementioned heptasaccharide.[17] The characteristic H-6a,b/C-6 crosspeaks of 4,6-linked β-Man*p* were very broad in the HSQC spectrum at 3.94–4.03, 3.79–3.84/67.3 ppm, but the methylene protons could not be correlated to the ring protons in the 2D spectra. The chemical shifts of a given backbone residue in acetylated polysaccharides vary significantly according to the nature of the sugars in the nearest-neighbor positions and the triad fragments indicated by these sequence-specific chemical shifts variations have also been collected in Table 2. The triad definitions have been given as a footnote to Table 2.

Chemical shift data for the 2- and 3-O-acetylated β-Man*p* units were easily extracted from the 2D spectra. Three sets of signals (referred to as major, weak, and minor components) were observed for both the 2- and 3-O-acetylated β-Man*p* residues. The signals of the H-2 (5.52, 5.49, and 5.42 ppm for M_{24} maj, M_{24} weak, and M_{24} min, respectively) and H-3 (5.13, 5.11, and 5.06 ppm

Table 3. Interresidue ROESY and HMBC data defining the glycosidic linkages of the water-soluble spruce galactoglucomannan

Sugar (x)	Preceding linkage (x+1)→(x)	Following linkage (x)→(x minus 1)	Triads
→4)-β-Man*p*-(1→, 2-*O*-Ac maj	H-1(M_4 maj)/H-3(M_{24} maj) m[a] $^3J_{C\text{-}1(M_y),H\text{-}4(M_{24}\ maj)}$[b]	H-1(M_{24} maj)/H-4(M_4 min2) m[a] H-1(M_{24} maj)/H-3(M_4 maj) or H-4(M_4 min1)	$M_4\underline{M}_{24}M_4$ $M_y\underline{M}_{24}M_4$
→4)-β-Man*p*-(1→, 2-*O*-Ac min	H-1(M_4 maj)/H-3(M_{24} min) m[a]	H-1(M_{24} min)/H-3 & H-4(M_{34} min) m[a] $^3J_{H\text{-}1(M_{24}\ min),C\text{-}4(M_4\ min1)w}$[b]	$M_4\underline{M}_{24}M_{34}$ $M_4\underline{M}_{24}M_4$
→4)-β-Man*p*-(1→, 2-*O*-Ac w		$^3J_{H\text{-}1(M_{24}\ w),C\text{-}4(M_4\ min2)\ w}$[b] H-1($M_{24}$ w)/H-4(M_x)	$X\underline{M}_{24}M_4$ $X\underline{M}_{24}M_x$
→4)-β-Man*p*-(1→, 3-*O*-Ac maj	$^3J_{H\text{-}1(M_4\ min2),C\text{-}4(M_{34}\ maj)}$[b] H-1($M_4$ min2)/H-3(M_{34} maj) w[a]	H-1(M_{34} maj)/H-3(M_{24} maj) m[a] H-1(M_{34} maj)/H-4(M_x) m[a] $^3J_{C\text{-}1(M_{34}),H\text{-}4(M_4\ maj)}$[b] $^3J_{H\text{-}1(M_{34}),C\text{-}4(M_4)}$[b]	$M_4\underline{M}_{34}M_{24}$ $M_4\underline{M}_{34}M_4$
→4)-β-Man*p*-(1→, 3-*O*-Ac min	H-1(M_{24} min)/H-4(M_{34} min) m[a]	H-1(M_{34} min)/H-4(G min) m[a]	$M_{24}\underline{M}_{34}G$
→4,6)-β-Man*p*-(1→		$^3J_{H\text{-}1(M_{46}),C\text{-}4(G)}$	$X\underline{M}_{46}G$
→4)-β-Man*p*-(1→maj	$^3J_{C\text{-}4(M_x),H\text{-}1(M_4\ maj)}$[b]	H-1(M_4 maj)/H-3(M_{24}) m[a] H-1(M_4 maj)/H-4(M_x) m[a] $^3J_{C\text{-}1(M_y),H\text{-}4(M_x)}$[b]	$G\underline{M}_4M_{24}$ $M_X\underline{M}_4M_X$
→4)-β-Man*p*-(1→min1 and min2	$^3J_{H\text{-}1(M_{24}\ min),C\text{-}4(M_4\ min1)w}$[b] $^3J_{H\text{-}1(M_{24}\ w),C\text{-}4(M_4\ min2)w}$[b]	H-1(M_4 min2)/H-3(M_{34} maj) w[a] H-1(M_4 min2)/H-4(M_{34} maj) m[a] $^3J_{H\text{-}1(M_4\ min2),C\text{-}4(M_{34})}$[b]	$M_{24}\underline{M}_4M_{34}$
→4)-β-Glc*p*-(1→maj	$^3J_{H\text{-}1(M_{46}),C\text{-}4(G)}$[b]	H-1(G) s[a]/H-4(M_x) $^3J_{H\text{-}1(G),C\text{-}4(M_x)}$[b]	$M_{46}\underline{G}M_x$
→4)-β-Glc*p*-(1→min	H-1(M_{34} min)/H-4(G min) m[a]	$^3J_{H\text{-}1(G),C\text{-}4(M_x)}$[b]	$M_{34}\underline{G}M_X$

Key: s, strong; m, medium; w, weak; residue designation—G, 4-linked Glc; M_{24}, 2-O-acetylated 4-linked Man; M_{34}, 3-O-acetylated 4-linked Man; M_4, nonacetylated 4-linked Man; M_{46}, nonacetylated 4,6-linked Man; M_x, M_4 or M_{24}; M_y, M_4 or M_{46}; X, unassigned.
[a]ROESY (τ_m 100 ms) crosspeaks.
[b]HMBC correlations.

for M_{34} maj, M_{34} weak, and M_{34} min, respectively) protons adjacent to the acetyl groups are strongly shifted to low field and give rise to isolated TOCSY crosspeaks that allow assignment of the ring protons and carbons. The chemical shifts were analogous to the partial data reported for specific triads containing (1→4)-linked glucose and mannose residues in acetylated glucomannan.[4] It is to be noted that the chemical shift assignments in the present study, albeit more complete, are almost identical to the partial assignments previously reported for spruce acetylated GGM.[14] The H-6a,b/C-6 crosspeaks of the mannose and glucose residues overlapped in the HSQC spectrum (a broad crosspeak encompassing the 3.61–4.10 ppm region in the proton dimension is detected at 61.5 ppm in the carbon domain).

2.2.2. Glucose. The (1→4)-linked β-Glc*p* residues gave two sets of H-1/H-2 (4.53/3.364 and 4.53/3.35 ppm, respectively, for the major and minor components) and H-2/H-3 crosspeaks in the DQCOSY spectrum. The H-1–H-5 connectivity was then completed from the very intense H-2/H-4, H-1/H-3, and H-1/H-5 correlations in the ROESY (mixing time 100 ms) spectrum (Fig. 4). The largest chemical shift variation between the two sets of β-Glc*p* signals in Table 2 was for H-4. It is to be noted that the set of carbon chemical shifts for β-Glc*p* (maj or min) is analogous to those reported for the glucosyl residue of GGM of *Picea abies* L. Karst.[18] However, strong H-2/C-3 crosspeaks in the HMBC spectrum indicated that the C-3 and C-5 chemical shifts should be reversed.

2.2.3. Galactose. A sharp H-1/H-2 crosspeak (5.038/3.83 ppm) was observed for the α-Gal*p* residue in the DQCOSY spectrum with the expected fine structure (small and large, $J_{1,2}$ and $J_{2,3}$ coupling) and identical chemical shifts to those reported for digalactosylmannopentaose.[17] Complete proton and carbon connectivity could be extracted from the HMBC spectrum (H-1/C-3, H-1/C-5, H-2/C-3, H-3/C-2, H-4/C-3, H-4/C-2, H-5/C-6, H-6/C-4).

Softwood GGM is traditionally described as substituted by only single α-Gal*p* units. Capek et al.[18] found indications of β-D-Gal*p*-(1→6)-Man*p* segments as well as of a (1→6)-linked galactosyl dimer in the deacetylated GGM, but more recently,[13] in a study of acetylated GGM, this was not reported. Some primary cell wall GGMs have, in fact, been shown to have both single galactosyl and β-arabinopyranosyl substituents[16] as well as β-Gal*p*-(1→2)-α-Gal*p*-(1→ disaccharides attached to Man*p* units.[6,16] Whether these Gal*p* dimers are incorpo-

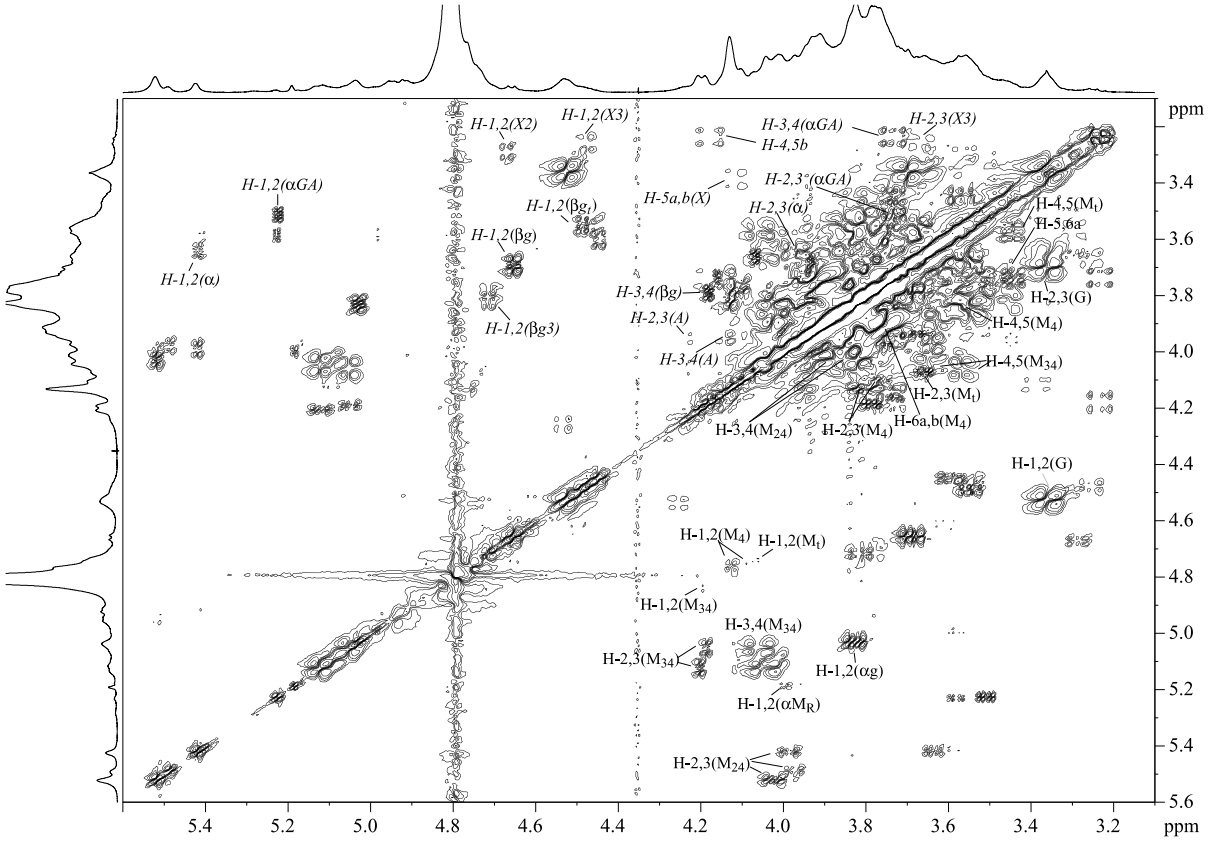

Figure 2. DQCOSY spectrum of acetylated GGM. The bottom right half contains labels of the sugar units belonging to the GGM polysaccharide, while the upper left half contains the labels for the minor hemicellulose impurities. Key as given in Figure 1.

rated in the GGM structure or exist as separate compounds is not clear due to the small size of the oligosaccharide fragments that were studied. Natural hemicelluloses are known to show structural diversity but such variations can be difficult to identify due to their limited occurrence or to the difficulty in distinguishing them from other minor hemicelluloses. One residue with chemical shifts analogous to those reported for β-Ara*p*-(1 → 6) Man*p*[16] displayed fairly strong crosspeaks in all the 2D spectra. However, from the large value of the $^{3}J_{\text{H-3,H-4}}$ coupling constant evaluated through the fine structure of H-3 in the H-2/H-3 DQCOSY crosspeak, it can be surmised that this sugar must have a *gluco* or *xylo* configuration (indicated as 'α' in the figures). Its chemical shift data have been included in Table 2 as it does not correspond to a glycosyl moiety of the hemicellulose contaminants isolated with the GGM.

2.3. Sequential analysis

The interglycosidic correlations found in both the HMBC and the ROESY spectra are collected in Table 3. All of the GGM backbone residues except M_{24} maj displayed crosspeaks from heteronuclear $^{3}J_{\text{H-1,C-4}'}$ coupling and these data were the most straightforward to interpret due to the relatively good spectral dispersion of the H-1 and C-4 signals. All of the sugars also exhibited intraresidue crosspeaks involving the anomeric carbons ($^{3}J_{\text{C-1,H-2}}$) that were useful probes for distinguishing the overlapping C1 chemical shifts of the nonacetylated β-Man*p* units. $^{3}J_{\text{C-1,H-4}'}$ crosspeaks were missing for M_{24} and β-Glc*p*. The HMBC data demonstrated the presence of the following disaccharide fragments: M_yM_{24}, $M_{24}M_4$, M_4M_{34}, $M_{34}M_4$, $M_{34}G$, $M_{46}G$, M_yM_x, M_xM_4, and GM_x.

As regards the ROESY data, the anomeric protons of the β-Man*p* (β-Glc*p*) sugars showed three (two) strong intraresidue interactions, namely H-1/H-2, H-1/H-3, and H-1/H-5 (H-1/H-3 and H-1/H-5) due to the corresponding very short (~2.5 Å) interproton distances. As a result, only ROE crosspeaks in nonoverlapping regions (preferentially with well-defined characteristic fine structure) could be used as sequential probes. Globally, the correlations in the ROESY spectra corroborated the HMBC data and new sequential correlations such as H-1(M_{24} min)/H-3 and H-4(M_{34} min) and H-1(M_{34} maj)/H-3(M_{24} maj) also indicated significant populations of the $M_{34}M_{24}$ and $M_{24}M_{34}$ diads,

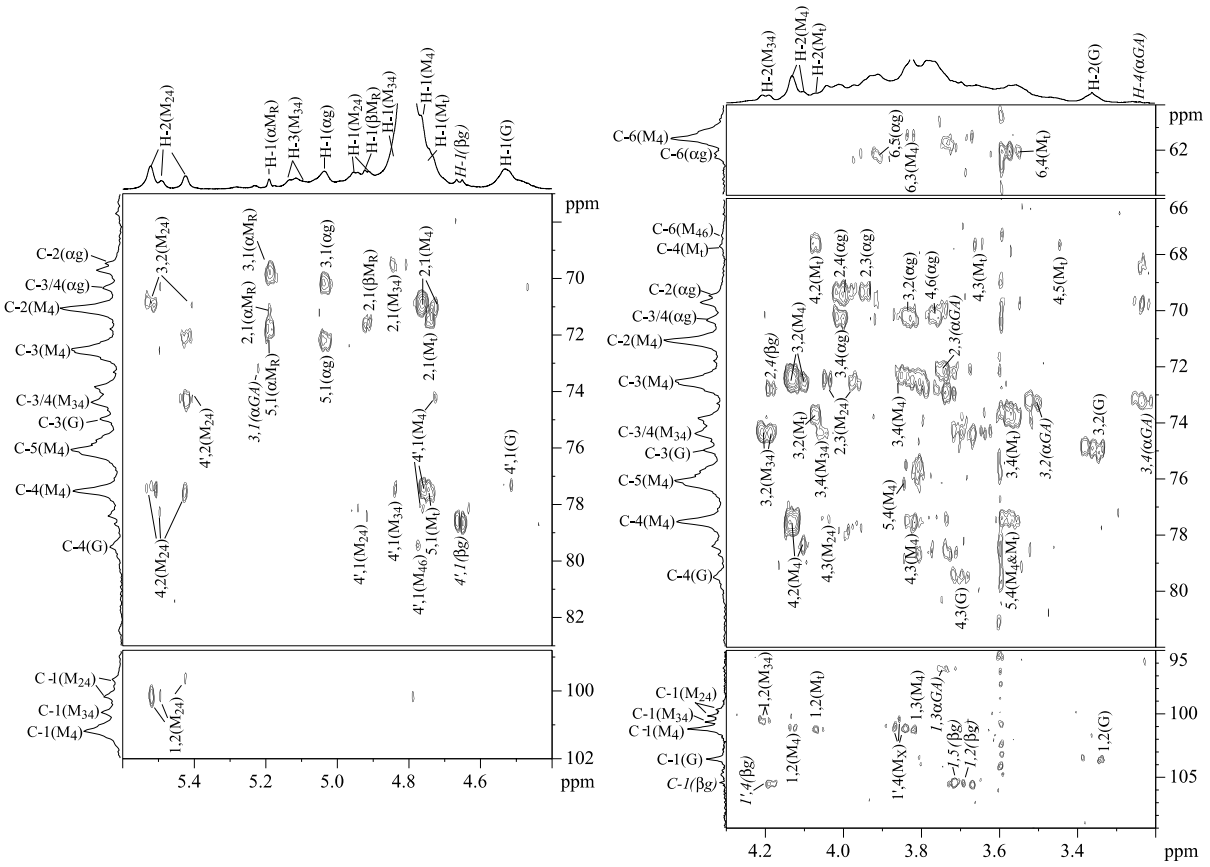

Figure 3. HMBC spectrum of acetylated spruce GGM. Correlations are given as C,H (sugar) while the prime symbol (′) indicates an interresidue bond. Key as given in Figure 1.

respectively. Finally, weak broad correlations between the anomeric proton of α-Gal*p* and the methylene protons of M_{46} (a broad crosspeak in the 3.75–4.05 ppm region interrupted by the strong H-1/H-2 crosspeaks) gave evidence of the α-Gal*p*-(1→6)-β-Man*p* linkage. The disaccharide fragments determined for GGM on the basis of the sequential correlations were grouped to give triads (i.e., for a given component such as M_{34} maj, the $M_4\underline{M}_{34}M_{24}$, and $M_4\underline{M}_{34}M_4$ triads could be proposed, last column of Table 3). This latter set of experimental triads is analogous to those in Table 2 that are based on chemical shift analysis alone. Thus, the sequence-specific chemical shift variations reported in acetylated glucomannans[4] are also found in GGM.

A dichotomy in the H-5 chemical shifts of the Man*p* (M_{24}, M_{34}, and M_4) residues ($\Delta\delta_{H\text{-}5} \sim 0.08$–$0.10$ ppm) has been observed in the present study. Perusal of the proton chemical shift data for galactomannans[17] shows that 6-substitution produces a downfield shift of the H-5 resonance. However, variations of the H-5 shift analogous to the ones in Table 2 have also been reported for acetylated glucomannans with very low amounts of galactosyl residues (<3%; the unassigned ^{1}H chemical shifts in the paper by Lundqvist et al.[14] can now be assigned in light of the data in Table 2). As the distance between H-2 and H-5′ of contiguous residues would be fairly short if the GGM backbone adopted a twofold helical arrangement, it seems probable that the variations in the shifts of the H-5 resonance are induced by *O*-acetylation. Moreover, it appears likely that the H-4 chemical shift variation ($\Delta\delta_{H\text{-}4} \sim 0.05$ ppm) between the major and minor glucosyl components is also related to the nature of the preceding sugar (3.63 and 3.68 ppm for the $M_{46}\underline{G}M_x$ and $M_{34}\underline{G}M_x$ triads, respectively).

All of the sequential NMR data depend upon the dihedral angles of the glycosidic linkage, Φ (C5–C1–O1–C4) and Ψ (C1–O1–C4–C5). From an experimental point of view, the amplitudes of the HMBC crosspeaks are modulated by trigonometric functions of the product of the heteronuclear vicinal coupling constants and the *J*-filter (65 ms). Thus, different orientations of the glycosidic linkages would be expected to afford different crosspeak intensities in the HMBC spectrum. It has been shown in a combined NMR and molecular modeling study[19] of a related β-(1→4)-linked xyloglucan heptasaccharide (α-Xyl*p* residues are substituted at C-6 of β-(1→4)-linked glucan) that both strong H-1/H-4′ and H-1/H-3′ NOE crosspeaks could be detected. These interactions were interpreted in terms of *syn* and *anti* conformers, respectively, which translate very different

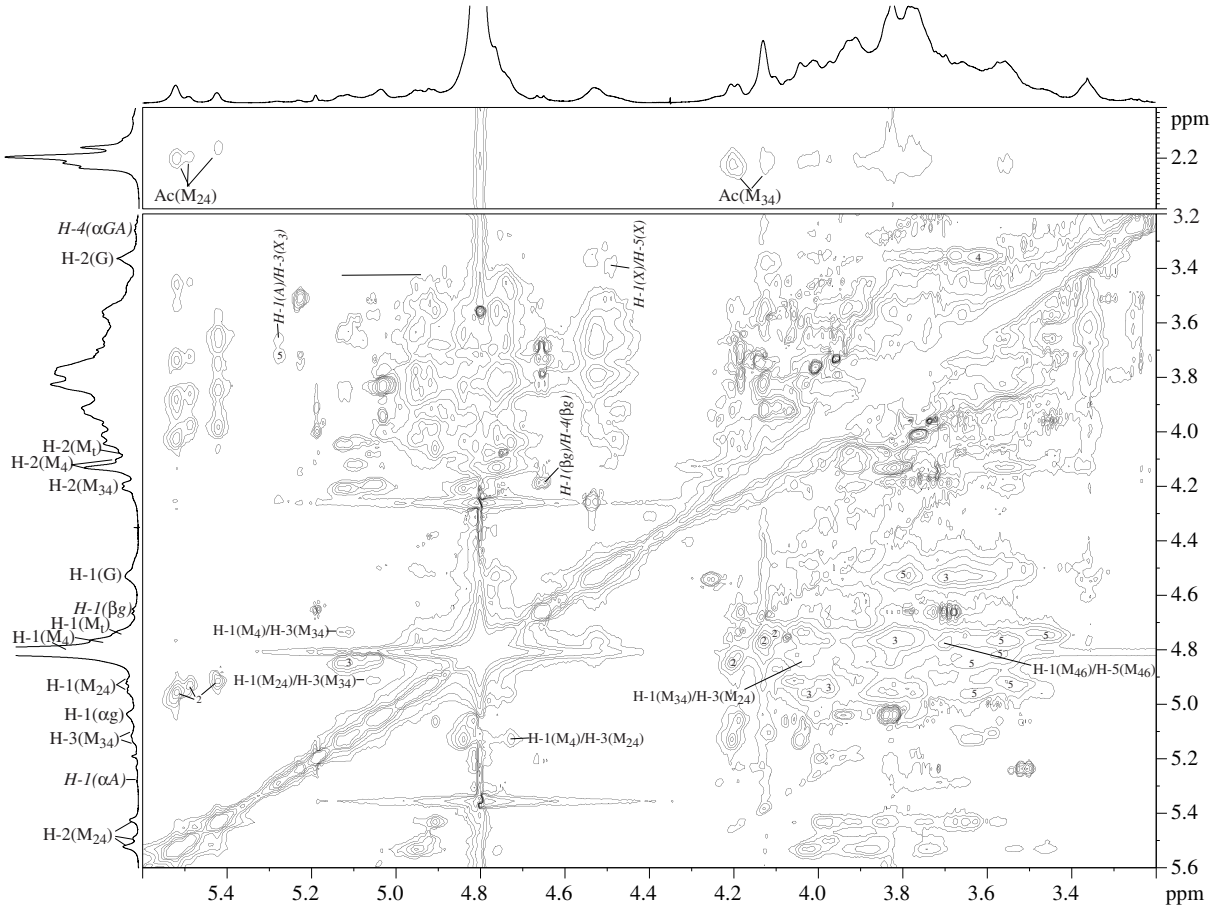

Figure 4. ROESY spectrum recorded with 100 ms mixing time. Some of the correlations listed in Table 3 and in the text are indicated. Key as given in Figure 1.

orientations about the glycosidic linkage. In the present study, the strong H-1/H-3′ interactions detected for M_{24} min suggest an important *anti* conformer population for this sugar. Finally, it should be noted that the acetyl groups of both M_{24} and M_{34} displayed strong intraresidue ROE crosspeaks with H-2 (the acetyl group of M_{34} did not present an intraresidue ROE with H-3).

In conclusion, all the NMR data infirm a blockwise distribution of the various sugars in GGM. Although some disaccharide fragments such as $\underline{M}_{46}G$ do seem characteristic of the fine structure of this polysaccharide, the residue distribution appears to be fairly random. This is in agreement with the irregular acetyl group distribution in galactoglucomannan and glucomannan that has been determined by chemical modification[20] and SEC/MALDI mass spectroscopy[21,22]. The sequence-specific chemical shift variations described above should prove useful in future studies of related polysaccharides. Full interpretation of the HMBC and ROESY data collected for acetylated GGM will require a state-of-the-art molecular modeling study. So far attempts to probe the GGM/hydrophobic molecule interactions with translational diffusion measurements and carbon relaxation parameters as a function of GGM concentration have not been successful (irreproducible data). However, the nature of carbohydrate/hydrophobic molecule interactions varies significantly with carbohydrate structure and future studies will require a more homogeneous GGM sample without the hemicellulose contaminants described below. Investigation of the stabilization of emulsions by dissolved mannans using other techniques where the stability of the droplets is measured quantitatively by GC analysis is presently under way.

2.4. Minor components

In the high yield GGM isolation procedure, it was not possible to totally eliminate other minor wood hemicelluloses. The isolated GGM in the present study was rather pure (93%). The results from GC analysis after acid methanolysis showed that the remaining part was mostly galacturonic acid (~3.5%), arabinose (~1.2%), xylose (1.3%), and glucuronic acid (<1%), indicating the existence of pectins, arabinogalactans and arabinoglucuronoxylans. Although these minor wood compounds

Table 4. ^{1}H and ^{13}C NMR data for minor polysaccharide groups in the isolated GGM

Polysaccharide Sugar	H-1 C-1	H-2 C-2	H-3 C-3	H-4 C-4	H-5a,b C-5	H-6a,b C-6	Ref.
Arabino glucuronoxylan							
α-Ara*f*-(1→3	5.275	4.235	3.955	4.15	3.72/		
	110.36	82.45	77.74	84.9	62.4		
→4)-β-Xyl*p*-(1→	4.5	3.32	3.58/3.52	3.81	4.12/3.39		24
	103.57	73.9	73.8/73.2	77.5	63.9		
→2,4)-β-Xyl*p*-(1→	4.664	3.29	3.63				
	101.17						
→3,4)-β-Xyl*p*-(1→	4.48	3.26	3.667				
	102.7	73.9	77.7				
α-Glc*p*A-(1→2	5.228	3.515	3.74	3.23	4.18[a]		
	96.57	72.29	73.386	73.007			
Arabinogalactan							
→3)-β-Gal*p*-(1→	4.72	3.81 (3.79)	3.895	4.24			27
	104.8	71.2	82.6				
→6)-β-Gal*p*-(1→	4.47	3.56 (3.61)	3.68	3.97	3.93		27
	104.63	71.8					
β-*Galactan*							
→4)-β-Gal*p*-(1→	4.659	3.69	3.79	4.19	3.73		28
	105.428	72.827	74.36	78.68	75.605		

Conditions as indicated in Table 1.
Weak proton and carbon *O*Me signals were observed at 3.47 and 60.8 ppm, respectively.
[a]Superposition of 2H-5 signals.

represent a very small fraction of the sample, they gave rather strong NMR signals due to their smaller molar mass. The chemical shifts of these components are given in Table 4.

2.4.1. Arabino-4-*O*-methylglucuronoxylan. The presence of α-Ara*f* residues (δ_{H1} 5.27 ppm) was revealed in the HSQC spectrum due to the characteristic ^{13}C chemical shifts. The H-1–H-2–H-3 connectivity was established from TOCSY crosspeaks in spectra with various mixing times and H-2–H-3–H-4 correlations were detected in the DQCOSY spectrum. Two ROEs involving the anomeric proton (5.27/3.72 and 5.27/3.68 ppm) were attributed to intraresidue (H-1/H-5) and sequential (H-1/H-3′) interactions, respectively.

Several sets of H-1–H-2–H-3 crosspeaks in the DQCOSY spectrum were assigned to β-Xyl*p* units by comparison with data reported for arabinoxylan,[23,24] acetylated 4-*O*-methylglucuronoxylan,[25] and glucuronoxylan.[26] Characteristic crosspeaks for H-5a,b/C-5 (4.12, 3.39/63.9 ppm) were detected in the HSQC spectrum. Finally, H-5a/H-5b crosspeaks in the DQCOSY and H-1/H-5b correlations in the ROESY spectrum completed the connectivity for the (1→4)-linked β-Xyl*p* unit. The two other β-Xyl*p* residues have been assigned to 3,4-Xyl*p* and 2,4-Xyl*p* from comparison of the H-1 and H-3 (shifted to low field in 3,4-Xyl*p*) chemical shifts with literature data.

Finally, the characteristic ^{1}H and ^{13}C chemical shifts of α-glucuronic acid were also detected in the 2D spectra (DQCOSY—H-1–H-5; HMBC—H-1, H-2, H-4/C-3, and H-3/C-1). Both the low intensity of the 4-*O*-methyl crosspeaks (3.47/60.8 ppm) and the strong H-4/C-4 crosspeaks at 3.24/73.0 ppm in the HSQC suggested that only a small fraction of these residues carried the 4-*O*-methyl substituent. The fine structure of the H-4/H-5 DQCOSY crosspeak pointed to two species with identical H-4 and slightly different H-5 chemical shifts. Sequential correlations for the →4)-[α-L-GlcA*p* (1→2)-]-β-Xyl*p*-(1→)-disaccharide fragment were not detected.

2.4.2. Arabinogalactan. Two other sets of H-1/H-2 crosspeaks in the DQCOSY spectrum (each group of crosspeaks actually corresponded to two overlapping crosspeaks) at 4.72/3.81(3.79) and 4.47/3.56 (4.46/3.61) ppm also displayed the fine structure of β-Gal*p* units. They could be assigned to (1→3)-linked β-Gal*p* and (1→6)-linked β-Gal*p* units of arabinogalactan, respectively, as these shifts were identical to those reported for arabinogalactan (AGP) from grapes.[27] Crosspeaks in the TOCSY spectra with various mixing times (20, 40, and 65 ms) allowed assignment of H-3 (3.895 ppm) and H-4 (4.24 ppm) of (1→3)-linked β-Gal*p*, which in turn afforded the characteristic C-3 shift (82.6 ppm) for the branch point carbon in the HSQC spectrum. The TOCSY spectra also allowed the assignments of H-3–H-5 of (1→6)-linked β-Gal*p*. Unfortunately, the H-3 chemical shifts of this sugar were identical to those of 3,4-linked β-Xyl*p* and therefore the expected interglycosidic NOE for the α-L-Ara*f*-(1→3)-β-Gal*p*-(1→6)-disaccharide fragment of arabinogalactan overlapped with that of the α-L-Ara*f*-(1→3)-β-Xyl*p*-(1→4)-disaccharide of arabinoglucuronoxylan as is discussed above.

2.4.3. (1→4)-linked β-Galactan. An isolated sharp doublet at 4.66 ppm ($^3J_{1,2} \sim 8$ Hz) with integrated intensity analogous to that of the reducing mannosyl residues could be assigned to the anomeric proton of (1→4)-linked β-galactan. Correlations in both the DQCOSY and HMBC spectra afforded ^{1}H and ^{13}C chemical shift data for the pyranosyl ring. Both heteronuclear vicinal coupling ($^3J_{H1,C4'}$) and interglycosidic NOEs (H-1/H-4′) confirmed the nature of the interglycosidic bond. These results are in accordance with those reported for (1→4)-linked β-galactan from *Linum usitatissimum* L.[4,17] and from a mung bean.[28]

3. Experimental

3.1. Acetylated galactoglucomannans

A previously isolated and purified acetylated GGM from thermomechanical pulp (TMP) manufactured from Norway spruce was used.[29] The molar ratio of between Gal:Glc:Man:Ac of the low-molar-mass GGM was determined by GC analysis after acid methanolysis according to Sundberg et al.[30]

3.2. Molar mass determination

The average molar mass of the GGM was determined on a multi-angle laser light-scattering apparatus (DAWN-DSP-F, WYATT Technologies) combined with a Waters GPCV 2000, having two Shodex columns (OH-PAC) in series. The GGM was dissolved in distilled water and filtered on 0.2 μm filters before analysis. The slightly different results compared to the previous study,[29] are probably explained by use of new columns.

3.3. NMR analysis

For the NMR experiments 20 mg of GGM was dissolved in 0.75 mL of D_2O (99.97%) and the solution was filtrated on 0.2 μm filter prior to the transfer into the NMR tube (∅5 mm). All data were processed with Bruker software. The chemical shifts were referenced to the C-1 signal of glucopyranose (103.548 ppm) and the H-2 signal of the 2-O-acetylated mannopyranose (5.423 ppm). In one experiment, an internal standard (DMSO: δ_H and δ_C, 2.74 and 39.74 ppm, respectively) was also added in order to quantify the actual amount sugar residues observed by NMR.

Quantitative ^{13}C spectra were recorded on a Bruker DRX 400 spectrometer (QNP probe) operating at 400.13 MHz for ^{1}H and 100.62 MHz for ^{13}C. The experiments were recorded with composite-pulse decoupling at 25 °C using a 90° pulse of 6.0 μs and a relaxation delay of 2 or 8 s. The spectral width was 19,084 Hz and 4*k* data points were acquired. One spectrum was also recorded at 60 °C in order to see if a better peak separation could be obtained.

The size of all 2D time-domain matrices was 2048×1024 ($f_2 \times f_1$) and they were recorded on a Bruker DRX 500 at 25 °C in the phase-sensitive mode (TPPI) with a 3004.8-Hz spectral width in the proton dimensions if not indicated otherwise. A 2D homonuclear phase-sensitive DQFCOSY (a 2048×512 matrix) was acquired with 80 transients per t_1 increment, a 90° pulse of 6.3 μs and a relaxation delay of 2 s. A TQF-COSY spectrum was acquired with 72 transients per t_1 increment, a 90° pulse of 6.3 μs, a relaxation delay of 2 s and a spectral width of 2500.0 Hz. Two rotating-frame nuclear Overhauser effect spectra (ROESY, 2.6 kHz spinlock field) were recorded with mixing times of 100 and 200 ms, respectively, and a relaxation delay of 2 s. The number of transients per t_1 increment was 96 and 72 with spectral widths of 2500.0 and 3205 Hz, respectively. Four total correlation spectra (TOCSY, 8.3 kHz spinlock field) were recorded with mixing times of 20, 40, 65, and 70 ms and a relaxation delay of 1.7 s. The number of transients per t_1 increment was 48. The spectral width of the TOCSY spectra with two shortest mixing times was 2500.0 Hz. A heteronuclear single quantum correlation spectrum (HSQC) was run on a Bruker DRX 400 with a spectral width of 10052 Hz in the carbon dimension, a 90° pulse width of 6.6 μs and a relaxation delay of 2.5 s. The number of transients per t_1 increment was 160. A proton-detected multiple-bond coherence spectrum (HMBC) was acquired with a 65-ms *J*-filter. The number of transients per t_1 increment was 192, the relaxation delay 1.8 s and the width of the 90° pulse 6.2 μs. The spectral width was 90,024 Hz in the carbon dimension. A double quantum gradient-enhanced (echo–antiecho scheme) spectrum was acquired with 96 transients per t_1 increment and a spectral width of 3205 Hz. The relaxation delay was 2.1 s and the width of the 90° pulse 6.4 μs. All the 2D data matrices were multiplied by a squared $\pi/2$-phase-shifted sine bell prior to zero-filling and Fourier transformation. Selective 1D DPFGSE experiments[31] were also recorded with inversion of peaks that were hidden by the residual HOD signal. The hard pulse, the selective pulse, the mixing time, and the relaxation delay were 6.25 μs, 80 ms, 200 ms, and 5 s, respectively. Some experiments were performed at 40° and 50 °C.

T_1 measurements (^{13}C) were also performed on a Bruker DRX 400 spectrometer using the inversion-recovery pulse sequence. Typically, nine spectra with T_1 delays ranging from 0.01 to 0.8 s were recorded with 6000 transients per spectrum, and a recycle delay of 2.204 s. The average T_1-value for three isolated methine signals was 335 ms. Upon twofold dilution, the T_1 did not notably change (360 ms). The T_1 of the acetyl group (carbonyls or methyls) was much longer (1.66 s).

For the analysis of hydrophobic interactions, approximately 5 mg of linoleic acid (*cis*-9, *cis*-12-octadecadienoic acid) (SIGMA) was mixed in alkaline D_2O (0.0225 mmol NaOH added) and different amounts of GGM was added (0.1, 1.2, and 5.5 mg). The mixture was filtrated on 0.2 μm filter before insertion into the NMR tube. Translational diffusion coefficients were determined according to Monteiro and Hervé du Penhoat.[32]

Acknowledgements

Dr. Miguel Angel Rodríguez Carvajal is gratefully thanked for help with informatics. Financial support from the international PhD Program in Pulp and Paper Science and Technology in Finland (PaPSaT) as well as the foundations 'Tekniikan Edistämissäätiö' and 'Ella och Georg Ehrnrooths Stiftelse' in Finland are gratefully acknowledged.

References

1. Annergren, G. E.; Rydholm, S. A. *Svensk Papperstidn.* **1960**, *63*, 591–600.
2. Sjöström, E. *Wood Chemistry: Fundamentals and Applications*, 2nd ed.; Academic: New York, 1993.
3. Fengel, D.; Wegener, G. In *Wood: Chemistry, Ultrastructure, Reactions*; de Gruyter: Berlin, Germany, 1984.
4. van Hazendonk, J. M.; Reinerink, E. J. M.; de Waard, P.; van Dam, J. E. G. *Carbohydr. Res.* **1996**, *291*, 141–154.
5. Eda, S.; Akiyama, Y.; Kato, K. *Carbohydr. Res.* **1984**, *131*, 105–118.
6. Schröder, R.; Nicolas, P.; Vincent, S. J. F.; Fischer, M.; Reymond, S.; Redgwell, R. J. *Carbohydr. Res.* **2001**, *331*, 291–306.
7. Thornton, J.; Ekman, R.; Holmbom, B.; Örså, F. *J. Wood Chem. Technol.* **1994**, *14*, 159–175.
8. Sundberg, K.; Thornton, J.; Pettersson, C.; Holmbom, B.; Ekman, R. *J. Pulp Pap. Sci.* **1994**, *20*, J317–J322.
9. Holmbom, B.; Åman, A.; Ekman, R. *Proceedings, 8th International Symposium on Wood and Pulping Chemistry*, Espoo, KCL, Finland, 1995, 597–604.
10. Hannuksela, T.; Fardim, P.; Holmbom, B. *Cellulose* **2003**, *10*, 317–324.
11. Sundberg, K.; Holmbom, B. *Pap. Puu* **1997**, *79*, 50–54.
12. Otero, D.; Sundberg, K.; Blanco, A.; Negro, C.; Tijero, J.; Holmbom, B. *Nord. Pulp Pap. Res. J.* **2000**, *15*, 607–613.
13. Capek, P.; Alföldi, J.; Lišková, D. *Carbohydr. Res.* **2002**, *337*, 1033–1037.
14. Lundqvist, J.; Teleman, A.; Junel, L.; Zacchi, G.; Dahlman, O.; Tjerneld, F.; Stålbrand, H. *Carbohydr. Polym.* **2002**, *48*, 29–39.
15. Willför, S.; Sjöholm, R.; Laine, C.; Roslund, M.; Hemming, J.; Holmbom, B. *Carbohydr. Polym.* **2003**, *52*, 175–187.
16. Sims, I. M.; Craik, D. J.; Bacic, A. *Carbohydr. Res.* **1997**, *303*, 79–92.
17. Davis, A. L.; Hoffmann, R. A.; Russell, A. L.; Debet, M. *Carbohydr. Res.* **1995**, *271*, 43–54.
18. Capek, P.; Kubačková, M.; Alföldi, J.; Bilisics, L.; Lišková, D.; Kákoniová, D. *Carbohydr. Res.* **2000**, *329*, 635–645.
19. Picard, C.; Gruza, J.; Derouet, C.; Renard, C.; Mazeau, K.; Koca, J.; Imberty, A.; Hervé du Penhoat, C. *Biopolymers* **2000**, *54*, 11–26.
20. Kenne, L.; Rosell, K.-G.; Svensson, S. *Carbohydr. Res.* **1975**, *44*, 69–76.
21. Jacobs, A.; Lundqvist, J.; Stålbrand, H.; Tjerneld, F.; Dahlman, O. *Carbohydr. Res.* **2002**, *337*, 711–717.
22. Teleman, A.; Nordström, M.; Tenkanen, M.; Jacobs, A.; Dahlman, O. *Carbohydr. Res.* **2003**, *338*, 525–534.
23. Hoffmann, R. A.; Kamerling, J. P.; Vliegenthart, J. F. G. *Carbohydr. Res.* **1992**, *226*, 303–311.
24. Baier, M.; Goldberg, R.; Catesson, A. M.; Liberman, M.; Bouchemal, N.; Michon, V.; Hervé du Penhoat, C. *Planta* **1994**, *193*, 446–454.
25. Teleman, A.; Lundqvist, J.; Tjerneld, F.; Stålbrand, H.; Dahlman, O. *Carbohydr. Res.* **2000**, *329*, 807–815.
26. Bazus, A.; Rigal, L.; Gaset, A.; Fontaine, T.; Wieruszeski, J. M.; Fournet, B. *Carbohydr. Res.* **1993**, *243*, 323–332.
27. Saulnier, L.; Brillouet, J. M.; Moutounet, M.; Hervé du Penhoat, C.; Michon, V. *Carbohydr. Res.* **1992**, *224*, 219–235.
28. Hervé Du Penhoat, C.; Michon, V.; Goldberg, R. *Carbohydr. Res.* **1987**, *165*, 31–42.
29. Hannuksela, T.; Tenkanen, M.; Holmbom, B. *Cellulose* **2002**, *9*, 251–261.
30. Sundberg, A.; Sundberg, K.; Lillandt, C.; Holmbom, B. *Nord. Pulp Pap. Res. J.* **1996**, *11*, 216–219.
31. Stott, K.; Stonehouse, J.; Keeler, J.; Hwang, T. L.; Shaka, A. J. *J. Am. Chem. Soc.* **1995**, *117*, 4199–4200.
32. Monteiro, C.; Hervé du Penhoat, C. *J. Phys. Chem.* **2001**, *105*, 9827–9833.